Journal of Earth Sciences and Geotechnical Engineering, Vol. 16, No. 3, 2026, 1-27
ISSN: 1792-9040 (print version), 1792-9660 (online)
https://doi.org/10.47260/jesge/1631
Scientific Press International Limited

New Drilling Targets Identified Through Analysis of Geophysical and Geochemical Data from the Gawana and Sorbon Haoussa Sectors (Liptako, Southwest Niger)

Abdoulwahid Sani[1]*, Hallarou Mallam Mamane[2], Mahamane Moustapha Sanda Chékaraou[3], Karimou Dia Hantchi[4] and Moussa Konaté[2]

Abstract

Gold exploration within the permit area held by OM Goldstone Resources (covering the Gawana and Sorbon Haoussa sectors) in Niger's Liptako mining province faces challenges common to the mining industry in Africa and elsewhere in the world: a decline in the discovery of new, economically viable deposits and the corresponding rise in exploration costs. Ground-based geophysical methods, combined with structural analysis and geological mapping, are now invaluable tools for enhancing the accuracy of exploration target selection and identifying potential drilling areas. A multi-technique methodological approach has been developed to identify areas with high mining potential. These include fieldwork, geophysics, and geochemistry investigations. Among these methods, ground geophysics provided important data to better characterise the study area. The geophysical work carried out as part of this study consisted of multi-frequency electromagnetic induction (EMI) surveys. Characterization and mapping of the subsurface electrical conductivity and magnetic susceptibility revealed various conductive veins, with variable alignments, that correspond to gold anomalies. The various conductive veins correspond either to acidic intrusive units (granodiorite/granite) and unmineralized quartz veins, or to

[1*] Department of Fossil Energy, National School of Engineering and Energy Sciences, University of Agadez, Niger. P.O. Box 199, Agadez-Niger. *Corresponding author.
[2] Department of Geology, Groundwater and Georesources Laboratory, Faculty of Sciences and Techniques, Abdou Moumouni University of Niamey. P.O. Box 10662, Niamey-Niger.
[3] Department of Disciplines Didactic, Faculty of Educational Sciences, Djibo Hamani University, P.O. Box 255, Tahoua-Niger.
[4] Department of Geology, Faculty of Sciences and Techniques, University Dan Dicko Dankoulodo of Maradi. P.O. Box 456, Maradi-Niger.

Article Info: *Received:* June 13, 2026. *Revised: September 11, 2026.*
Published online: September 14, 2026.

sulphide-rich metasediments and grey quartz veins. Furthermore, the abundance of resistive units on the high-frequency map reveals intense weathering of the outcropping rocks; in the field, these correspond to alluvium derived from the weathering of manganiferous schists, as well as heavily weathered, sulfide-rich quartz veins. Consequently, the Gawana and Sorbon Haoussa sectors, located on the eastern edge of Niger's Liptako province, are expected to attract increased interest from gold exploration and development companies operating in the country.

Keywords: Gold mineralisation, Geophysical surveys, New drilling targets, Gawana and Sorbon Haoussa sectors, Liptako province of Niger.

1. Introduction

The discovery of new metallic mineral deposits, particularly gold, has declined globally, while exploration costs have risen significantly in recent years (Groves *et al.,* 2015). Such a global scenario compels exploration teams to increase their precision through more rigorous target selection and a reduction in costs associated with geological drilling (Gaboury, 2019, Noura *et al.,* 2024; Chen *et al.,* 2025; Harris *et al.,* 2025; Yechang *et al.*, 2025; Ouedraogo *et al.,* 2026). Groves *et al.,* (2015) reported, among other things, that in areas with little or no prior exploration, exploration teams often face a lack of both geological information and information regarding potential signs of mineralisation. This observation is all the more pertinent given that the selection of target zones must rely on the use of conceptual models based on the mineral system concept, which must be applied at the provincial scale (Echague *et al.,* 2024). Groves *et al.,* (2020) emphasize that these models must take into account parameters such as the geological setting, the geodynamic context, and the preservation of the mineral resource. Furthermore, the question of scale is an important parameter in this analysis. Indeed, the various types of gold deposits (e.g. orogenic gold, Carlin-type deposits, iron oxide-copper-gold (IOCG) deposits, and intrusion-related gold deposits (IRGDs)) exhibit distinct characteristics when analysed individually. However, on a global scale, they may have formed within the same geodynamic setting.

As in many West African countries, gold exploration and mining in Niger have been largely ignored due to the country's over-reliance on uranium as its main source of revenue. The country's gold production began in 2004 with "Société des Mines du Liptako" (SML), a subsidiary of the Canadian company SEMAFO, operating a gold mine at Samira ore deposit (better known as Samira Hill) in western Niger. To date, it remains the only ore company to exploit this resource on an industrial scale in the country. Gold prospecting has also been hampered by a lack of substantial funding and, above all, political commitment. The absence of systematic development and organized exploration has resulted in intense artisanal work targeting primary quartz-gold veins and related alluvial deposits in several regions of the country, notably the Liptako province. Recently, the global COVID-19 pandemic, falling uranium prices, and a new political will on the part of the authorities have prompted the country to consider diversifying its economy towards other mineral resources (such as gold, copper, tin, lithium, etc.) and reducing its dependence on uranium receipts.

Gold is one of the world's most valuable commercial mineral resources (Butterman *et al.,* 2005). In Niger, the greenstone belts are mainly considered to host gold mineralisation, notably the contact zones between these greenstone belts and granitoid plutons (Machens, 1973; Machens 1961; Soumaila and Konate, 2005). Also, previous studies in both Niger and Nigeria have linked gold mineralisation to geological structures controlled by hydrothermal alteration processes (Garba, 1988; Pour *et al.*, 2013). Since hydrothermal alteration structures and zones are of interest for gold prospecting, it is necessary to delineate geological structures that can serve as conduits for the remobilization and reworking of mineralizing fluids that concentrate the gold deposit (Boubacar Abdou, 2023; Gnamou *et al.,* 2023; Noura *et al.*, 2024). This is why geophysical methods have become necessary, as they measure variations in physical properties at, below, or near the Earth's surface (Kearey *et al.,* 2002). It should also be noted that spatial prediction of mineral resources is an essential element in effective resource exploration and management. According to Dentith and Mudge (2014), various variables that influence the presence of minerals in a geologically acceptable environment can be used to make predictions. These aim to focus future exploration efforts on promising areas where investment in time and resources will yield the best results, as well as geological mapping of mineralisation potential, constitute pioneering work that is frequently carried out as part of current exploration programs.

The western part of Niger is well known for its gold mineralisation contained in the Birimian formations of the Niger Liptako (Projet NER/88/023, 1991; JICA, 1993; Bossière *et al.,*1996; PADEM Projet, 1995 et Claude et Souleymane, 2010). It is worth noting that the term Birimian was first introduced by Kitson in 1928, during his study of the geological formations of the Birim Valley in Ghana (Soumaila, 2000; Soumaila and Konate, 2005). The term covers formations ranging in age from 2600 Ma to 1600 Ma. The Liptako province of Niger consists of alternating granitoid plutons and greenstone belts (Machens, 1973; Soumaila, 2000). The greenstone belts are represented, respectively, from NW to SE, by the Gorouol, Diagourou-Darbani, and Sirba greenstone belts (Soumaila and Konate, 2005). The present study focuses on the Sirba greenstone belt, more specifically, the Gawana and Sorbon Haoussa sectors. It should be noted that for decades, gold mining exploration has focused on the Birimian greenstone belts, whose associated deposits are now better studied. Previous studies carried out between 1992 and 1994 failed to identify areas with high gold potential. In recent years, despite the insecurity issues that have drastically affected the area, occasional research work has revealed new targets in the Sirba greenstone belt (Abdoulwahid and Souley, 2023). Gold in granitoids is also a recent discovery, and the parameters that characterise it remain poorly understood (Boubacar Abdou, 2023).

This study aims to identify new drilling targets based on geochemical and geophysical data analysis. This will enable the characterization of the mineralisation's host rock and the nature of the ore. Analysis of the structural characteristics of the deposit will help to determine the factors controlling the mineralisation. The methodology used consisted of a literature review combined with fieldwork, which enabled us to characterise the geology of the study area.

2. Site Presentation

The study area is located approximately 55 km northwest of Niamey, the capital of Niger (Fig. 1). It encompasses two sectors, Gawana and Sorbon Haoussa covering an area of approximately 1,562 km² (Fig. 1). Straddling the left and right banks of the Niger River, this area exhibits significant gold indications (JICA, 1993; PADEM Project, 1995; Claude et Souleymane, 2010) that are exploited on an artisanal basis using systematically aligned trenches targeting gold-bearing zones.

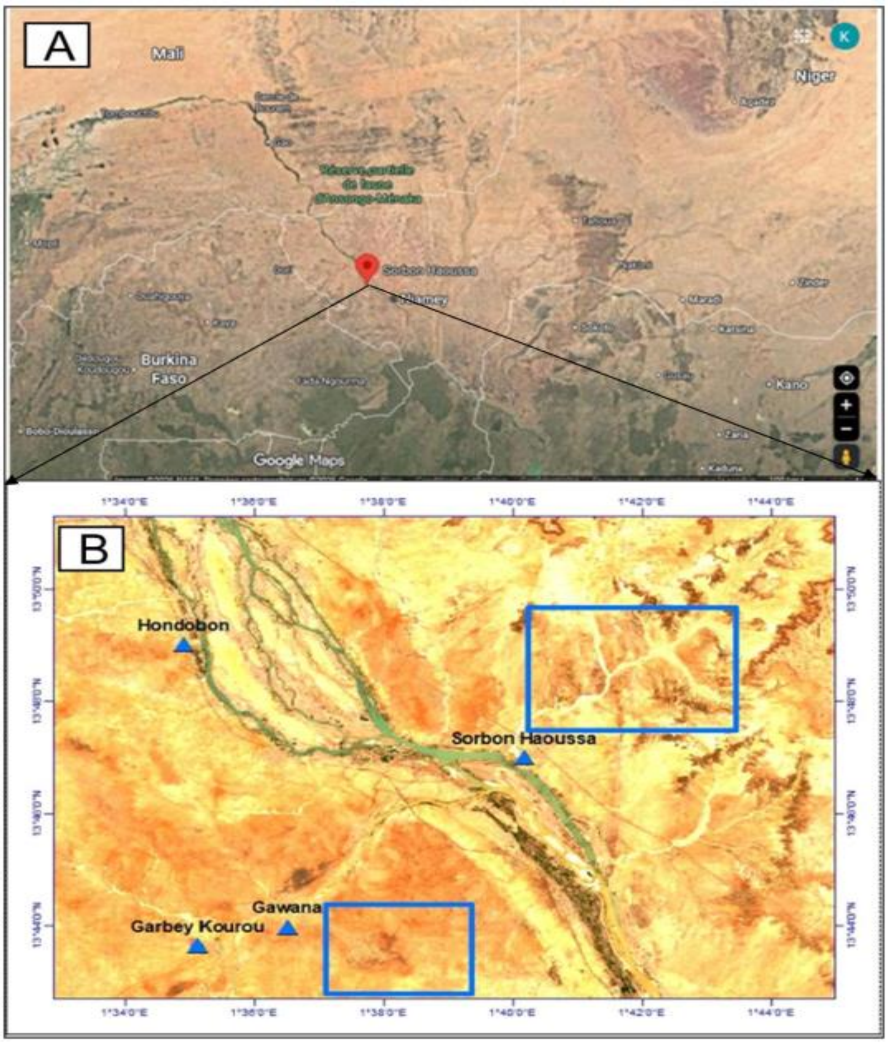

Figure 1: (A) Maps showing the location of Sorbon Haussa in the SW of Niger, and (B) localisation of the studied areas (blue dials).

Geologically, the Gawana and Sorbon Haussa sectors extend along the extreme northeastern margins of the Sirba greenstone belt, within the Liptako province of Niger (Fig. 2). This area is made up of alternating granitoids and greenstone belts. These greenstone belts consist of metabasalts, amphibolites, mafic-ultramafic bodies locally converted into talc schists and chlorite schists, weakly metamorphosed sediments, and small stocks of intermediate to acidic plutonic or volcanic rocks. The Liptako province of Niger (Fig. 2) is the northeastern part of the Man Shield, which is a component of the West African Craton.

The West African Craton consists of a Precambrian basement dated from the Lower to Middle Proterozoic (Kitson, 1928; Rocci, 1965; Trompette, 1973; Bessoles, 1977, Vachette, 1986; Palacky, 1987; Perrouty et al., 2012) with a sedimentary cover ranging in age from the Mesoproterozoic to the Cenozoic, infilling the basins of Taoudenni, Tindouf, Volta, and Iullemmeden (Naba *et al.,* 2004; Miningou *et al.,* 2017; Konaté *et al.,* 2018; Garba Saley *et al.,* 2024). The West African Craton, stabilized since 1700 Ma (Naba, 2007), is made up of two ridges: the Réguibat shield in the North and the Léo-Man shield in the South, with Kédougou-Kéniéba and Kayes inliers, in an intermediate position between the two shields (Kouamelan, 1996; Naba, 2007; Lompo, 2009).

According to Garba Saley *et al.,* (2024), in each of these shields, Archean formations to the West, and Paleoproterozoic (Birimian) formations to the East, can be distinguished. The best manganese mineralisations investigated in Niger are related precisely to the Birimian domain (Paleoproterozoic), in the Liptako area. The Niger Birimian domain extends along the western bank of the Niger River. It is composed of three main greenstone belts (Gorouol, Diagorou-Darbani, and Sirba), which consist of metasedimentary and metavolcanic formations trending NNE-SSW to NE-SW, intersected by vast granitoid plutons (Ama Salah, 1991; Noura, 2024).

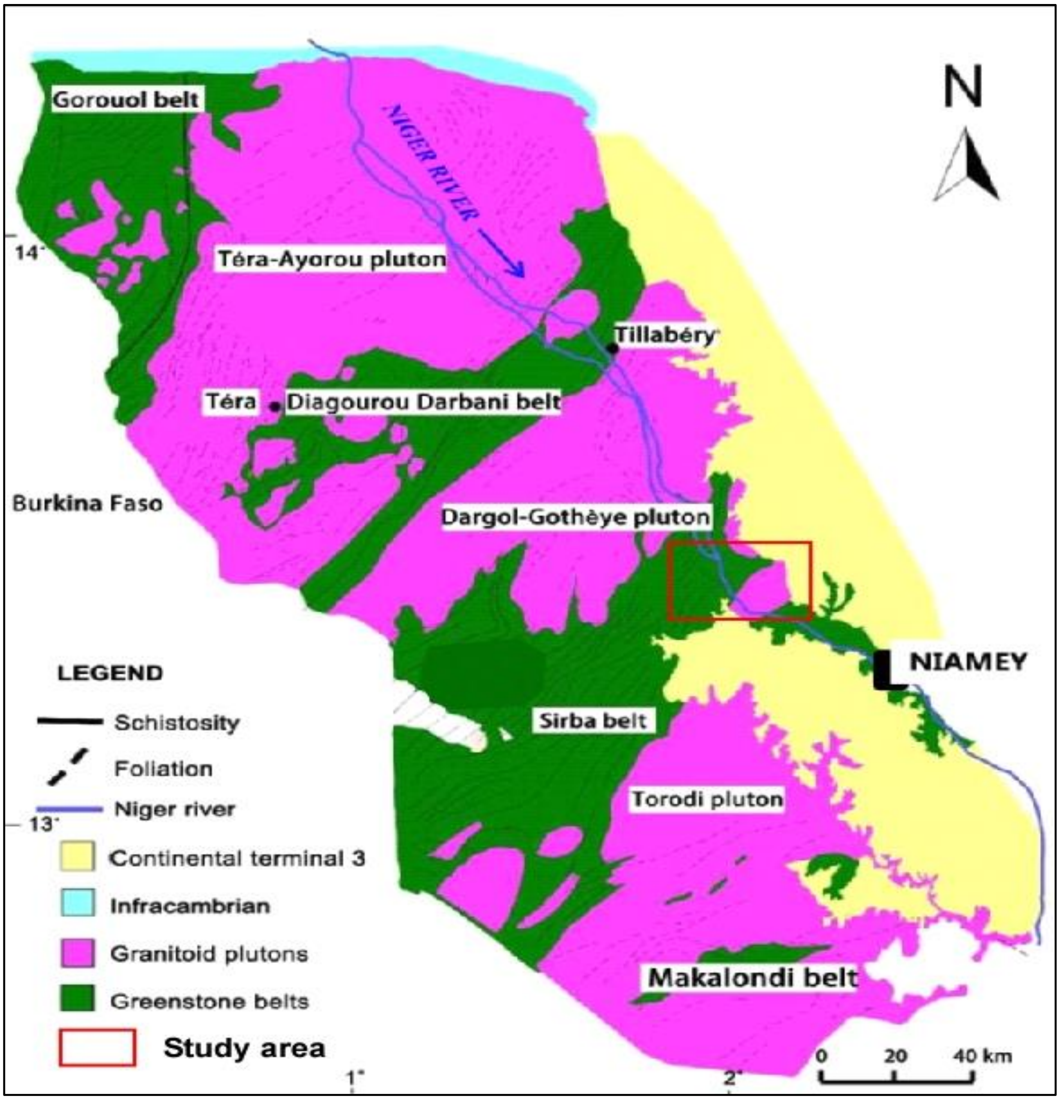

Figure 2: Geological map of the Liptako showing the studied area (modified from Noura et al., 2024).

3. Methods

The methodological approach adopted in this study primarily comprises a literature review, followed by fieldwork, geophysical surveys, and geochemical analyses.
The literature review aims to produce a geological synthesis. It should be noted that no large-scale scientific study has yet been conducted in this area.
Fieldwork involved the study of outcrops to update the geological map of the study area.
The geophysical work carried out as part of this study employed the multi-frequency electromagnetic induction method.
These surveys were used to map conductive and resistive units, which were interpreted in relation to mineralised zones and host rocks respectively, as well as

the directions, thicknesses, and depths of anomalies. In this study, multi-frequency electromagnetic surveys were mainly used to detect and map variations in conductive units in the subsoil (conductive veins, fractures, etc.).

The general operating principle is described below. When an electromagnetic wave penetrates the ground, it induces eddy currents in any conductive body (Faraday's law of induction), which then generates a disturbing magnetic field (Ampère's law) relative to the primary magnetic field of the transmitter. At the level of the receiver, the primary field Hp and the secondary field Hs are recorded.

The system used in this work is a PROMIS-10, a new multi-frequency electromagnetic induction technology that can send up to 10 frequencies, up to 28,160 Hz and 56,320 Hz for high frequencies. The other frequencies are 110 Hz, 220 Hz, 440 Hz, 880 Hz, 1760 Hz, 3520 Hz, 7040 Hz, and 14080 Hz. In addition, this system can record secondary magnetic fields along three X, Y, and Z axes.

Measurements are made profile by profile. At each measurement station, the system automatically switches from one frequency to another, which enables vertical sounding. We thus characterise the subsoil horizontally and vertically along each profile. This allows a two-dimensional representation of the subsurface to be obtained. The parameters measured at each station are the components in phase and the components in quadrature of the primary and secondary fields and the resistivity. These components are extracted electronically and presented as a percentage. Other parameters are also measured. The depth of investigation varies according to the transmission frequency, the resistivity of the medium, and the transmitter-receiver distance. The depth of investigation depends on the transmitted frequency, subsurface resistivity, and transmitter–receiver geometry. The effective depth of investigation should therefore be established for each frequency and survey configuration.

Geochemical analyses were conducted to confirm or rule out the presence of gold in high-potential zones. JICA's geochemical data were also superimposed on the new geochemical and geophysical data. This provided the basis for delineating the drilling zones.

The geochemical analysis, conducted as part of this study, consisted of determining gold concentrations using a shaking table at the Mining and Environmental Engineering Laboratory of the Niger School of Mines, Industry, and Geology (EMIG Niger). This table is used to process particles with diameters ranging from 75 µm to 4.75 mm. To make the separation process more efficient, the difference in density between dense and light particles must be exactly 1 g/cm^3.

It should be noted that it is the shaking action that causes the separation of particles into distinct groups, one of which has a high density and the other a low density. The light particles are removed by transverse movement, via a water jet for washing, where they are collected, while the heavy particles are conveyed longitudinally to the end of the table due to the direction and asymmetric nature of the shaking. The light particles are first examined before being discarded. For the heavy particles, the light elements are removed, followed by drying and weighing to determine the mass of the target substance (gold) expressed in g/t.

4. Main Results

4.1 Geological mapping of the study area

Except for the work of Abdoulwahid and Souley. (2023), the main work carried out has been limited to airborne geophysical prospecting campaigns (PADEM Projet, 1995) and geochemical analyses (JICA, 1993; PADEM Projet, 1995; Claude et Souleymane, 2010). This geophysical prospecting and geochemical work did not enable us to establish a geological map of the study area, or even better, to highlight potentially gold-rich zones. As part of the Niger Liptako gold project, fieldwork, geophysics, and geochemistry were carried out on the Sorbon Haoussa and Gawana target sites. These sites comprise three sub-sectors of varying sizes: 21 km^2 for Sector 1, 8 km^2 for Sector 2, and 1 km^2 for Sector 3. This has enabled us to produce a geological map of the study area (Fig. 3). The area features a variety of Precambrian geological formations. These formations are characterised by a diversity of rock outcrops: magmatic, metamorphic, and metasediments.

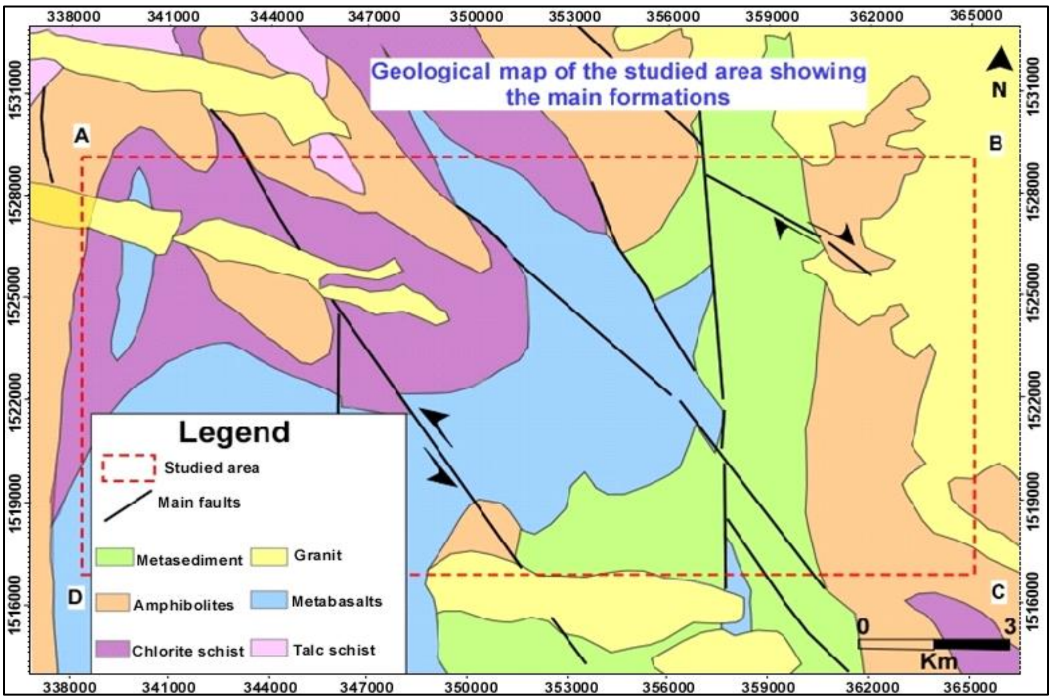

Figure 3: Geological map of the study area.

It should be noted here that the study area (Gawana and Sorbon Haoussa) is located in the northeastern part of the Sirba volcano-sedimentary belt (Fig. 2), one of the three Birimian (Early Proterozoic) greenstone belts in southwestern Niger. The main geological units of this area consist of metabasalts, amphibolites, talc schists and chlorite schists, metasediments, granitic batholite, and volcano-sedimentary formations (Fig. 3).

This observation is all the more pertinent given that the petrostructural analysis reveals a diversity of rocks and structures:
Talc schists (Fig. 4a): exhibiting two planes of schistosity (S1: N40°P77°NW and S2: N140°P75°E).
Metabasalts: with a shiny black colour due to the presence of amphibole needles, while the green colour is due to the presence of chlorite. An alternation of coarse to fine facies with fractures N85°P62°N was noted. Coarse metagabbros (Fig. 4f) with well-deformed centimetric crystals and chlorite recrystallizations were also observed.
Amphibolites are interbedded with metabasalts and chlorite schists in the NW, while in the E and SE, they occur as panels associated with granites. These rocks are dark gray to blackish, with fine, medium, and rarely coarse crystals. They are affected by S1 schistosity and are sometimes folded, dipping to the NE or SW.
Granites (Fig. 4h): with a grainy texture, exhibiting slightly oriented minerals, with a N38° trending foliation and dipping 88° towards the NE. These granites are distributed across the NW, E, SE, and NE parts of the study area. Quartz veins were also observed in the study area (Fig. 4c).
Metasediments or metavolcanosediments: these include metagreywackes (Fig. 4g), seritoschists, schists, quartzites (Fig. 4€), and chlorite schists (Fig. 4(b) &(d)).

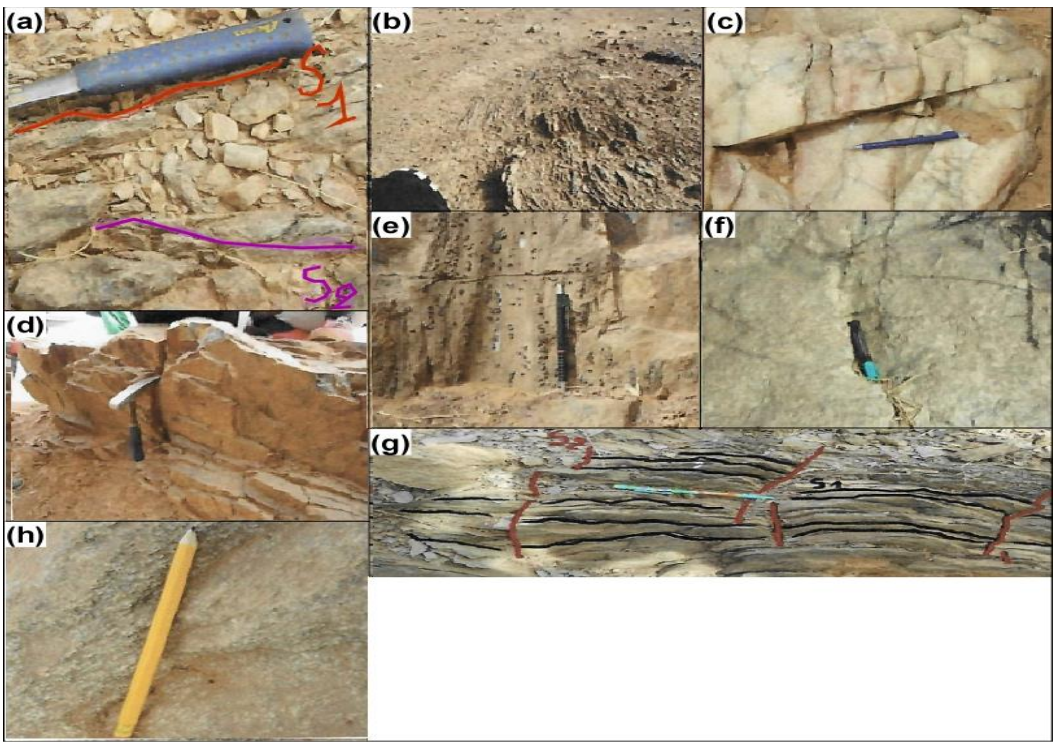

Figure 4: Petrographic facies in the study area. (a) talc schists, (b, d) chlorite schists, (c) quartz vein, (e) quartzites, (f) metagabbros, (g) metagreywackes, and (h) granite.

4.2 Structural analysis of the study area

According to the structural analysis of the study area, observations were made at 91 points to cover the entire area studied. It should be noted that the geological study allowed us to identify three major geological units. These geological units occur in alternating sequences across the study area: felsic intrusives (granitoids), Volcano-sedimentary formations, and mafic dykes cutting the felsic formations.

In the study areas, some rocks are deformed with a mineral lineation. The volcano-sedimentary formations are generally affected by shearing zones and are greatly weathered. From where the onset of lateralisation is observed at the surface of the outcrops. In the southeastern part, in contact with the granitoids, the volcano-sedimentary formations tend to change from a fine texture to a micro grained texture, due to the onset of crystallisation caused by the contact. To the northwest, they are more basaltic (volcanic). Mafic dykes were observed on a felsic intrusive in the NE part of the study area. These dykes have the same N-S trend as the granite massif. The geological structures are mainly dominated by shear zones over the entire studied area (Fig. 5). There are also faults, fractures, quartz veins, and a large-scale folding deduced in the studied area (Fig. 5a&b). Several fracture directions were observed. These are the following directions: E-W, N-S, NW-SE, and NE-SW. Faults and lineations orientations are generally N-S and NW-SE, with striae azimuth N30° to N90°, dipping gently to the NE or to the E.

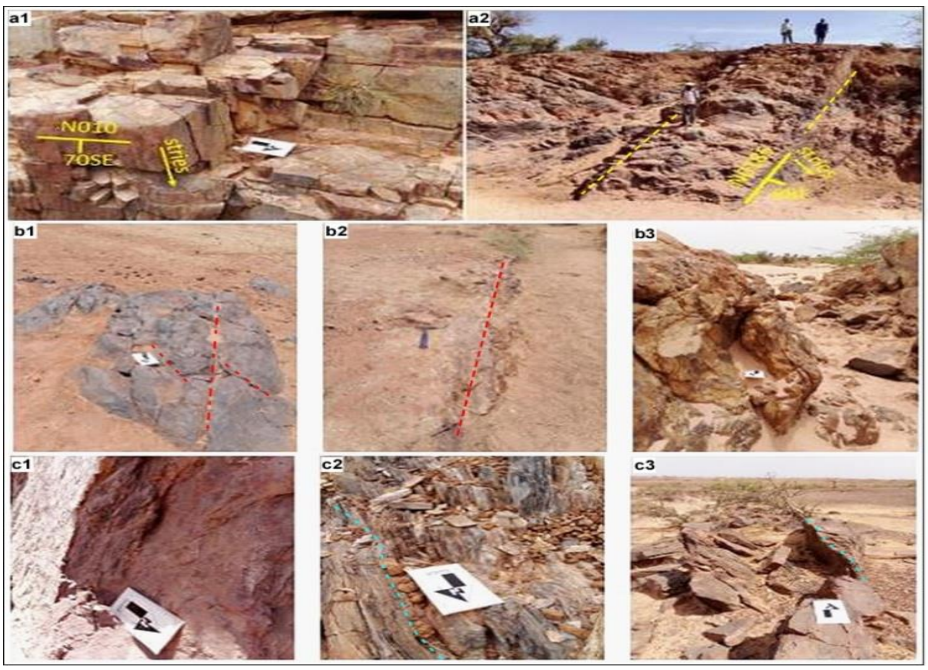

Figure 5: Photographs of the main tectonic structures within the study area. a&b fractures and faults, c: shearing deformations. a1: fracture N10°P70°NE, a2 : fault N185°P60°E, b1: fractures NW-SE, and NE-SW, b2: fault zone in contact with granite, b3: fault N165°P60°SW, c1: fault N340°P70°NE, c2: shear zone N350°P60NE, and c3: N-S trending shear zone.

Quartz veins are mostly associated with shear zones. They are boudinaged in this case. The quartz veins observed are generally oriented E-W, N-S, NW-SE, and NE-SW. The shear zones have generally NNW-SSE or NS trending (Fig. 5c). The few rare NW-SE and NE-SW trending shear zones observed are generally in the metavolcano-sediments or close to the granitoid contacts. Structural data analysis using stereonet yielded the results shown in the figure below.

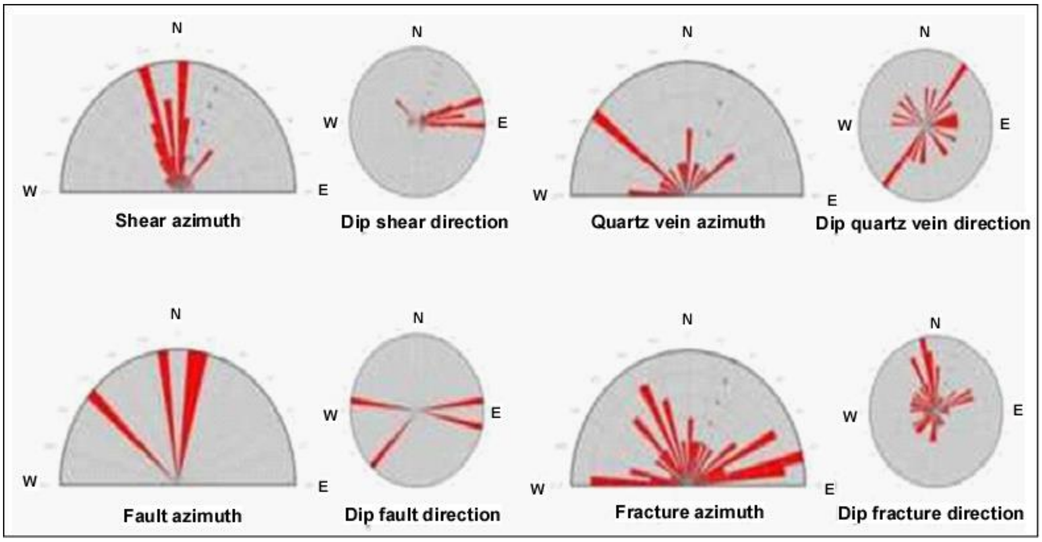

Figure 6: Structural data analysis using a stereonet.

4.3 Topographic variation analysis

The various sectors studied were positioned on the JICA anomaly map (Fig. 7a). Analysis of the topographic maps of the three Sectors enabled us to locate the high and low areas. The variability of the topography in sector 1 (Fig. 7b) shows the highest points to be to the east and extreme northwest, with altitudes ranging from around 220 m to 260 m, giving a maximum difference in altitude of around 40 m. In Sector 2 (Fig. 7c), altitudes decrease from SE to NW, down towards the SIRBA. The maximum elevation difference is approximately 52 m. Within sector 3 (Fig. 7d), the topographic variability increases from SE to NW, with a maximum vertical drop rarely reaching 22 m.

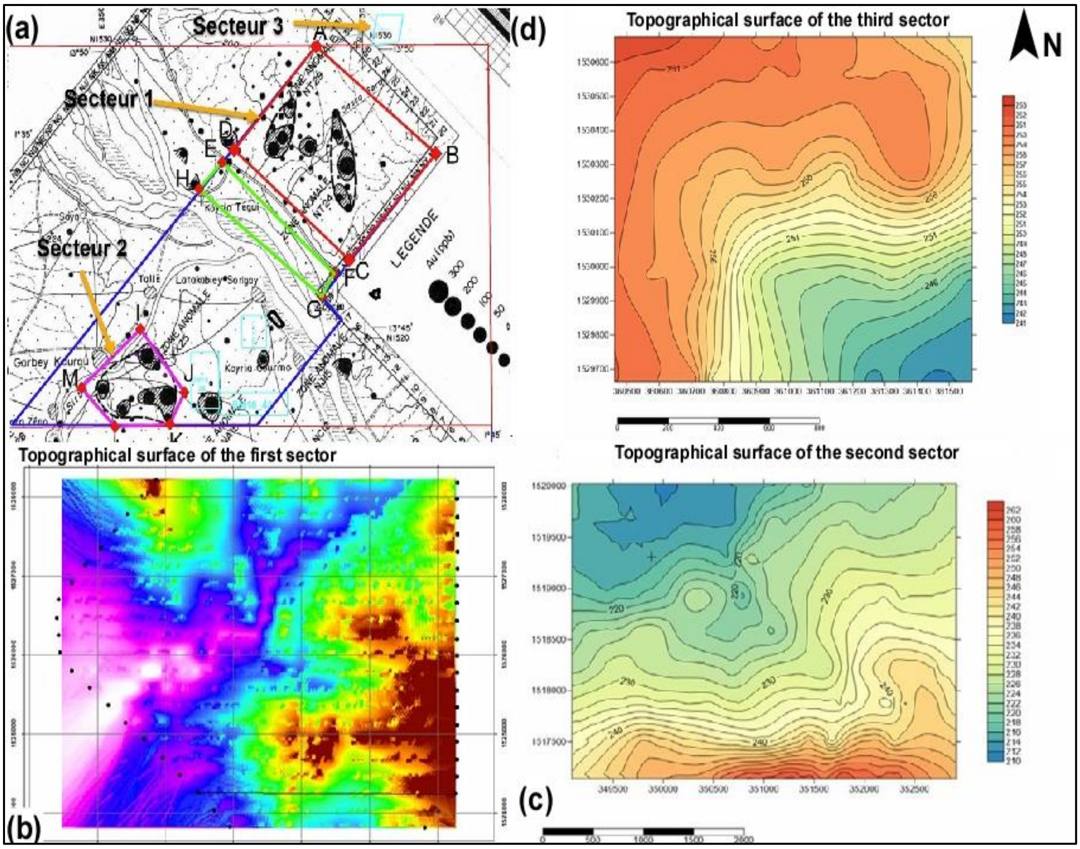

Figure 7: Topography map of the various parts of the study area. (a) Location of the three zones on the JICA (1993) anomaly map, (b) Sector 1, (c) Sector 2, and (d) Sector 3.

4.4 Geophysical data analysis

It should be noted that the geophysical work carried out in each sector as part of this study corresponds to the multi-frequency electromagnetic induction survey. Plane electrical resistivity values (profiles 8 to 14 for sector 1) and apparent electrical resistivity maps obtained by IDW are presented for low frequencies (110, 220, 440, and 880 Hz), medium frequencies (1,760, 3,520, and 7,040 Hz), and high frequencies (14,080, 28,520, and 56,320 Hz) for all sectors studied. The survey grid consists of 21 parallel lines running E-W for Sector 1, 9 parallel lines running E-W for Sector 2, and 5 parallel lines running E-W for Sector 3. The measurement points (stations), spaced 50 m apart, are marked by wooden stakes and surveyed using DGPS. The results of the electromagnetic survey are broken down as follows:

- Total number of profiles (all sectors combined): 35 ;
- total length of profiles: 129,800 m or 129.80 km;
- total number of measurements: 2624.

The table below gives a summary of the work carried out by Sector.

Table 1: Results of the electromagnetic survey carried out in the three sectors.

Sector 1			**Sector 2**		
Profiles	**Measurement points**	**Profile length (m)**	**Profiles**	**Measurement points**	**Profile length (m)**
Profil1	56	2,800	Profil1	42	2,050
Profil2	65	3,200	Profil2	57	2,800
Profil3	75	3,700	Profil3	69	3,400
Profil4	80	4,000	Profil4	74	3,800
Profil5	86	4,300	Profil5	78	3,850
Profil6	90	4,500	Profil6	62	3,050
Profil7	97	4,800	Profil7	39	1,900
Profil8	102	5,050	Profil8	32	1,550
Profil9	107	5,300	Profil9	14	650
Profil10	113	5,600	Total	467	23,050
Profil11	115	5,700	**Sector 3**		
Profil12	116	5,750	**Profiles**	**Measurement points**	**Profile length (m)**
Profil13	113	5,600			
Profil14	116	5,750	Profil1	24	1,150
Profil15	113	5,600	Profil2	24	1,150
Profil16	109	5,400	Profil3	24	1,150
Profil17	104	5,150	Profil4	24	1,150
Profil18	104	5,150	Profil5	24	1,150
Profil19	96	4,750	Total	120	5,750
Profil20	92	4,550			
Profil21	88	4,350			
Total	2,037	101,000			

4.4.1 Geophysical results in Sector 1

In sector 1, the geophysical results show that the resistivity anomalies (conductive anomalies) are characterised by their low resistivity values (red/green colours). The three maps (Figs. 8a, b, and c) show a north-south trending structure crossing profiles 8, 9, 10, 11, 12, and 13, totalling 880 m in length. Figure 7a also shows an east-west structure on profile 11, with a length of 5,700 m .

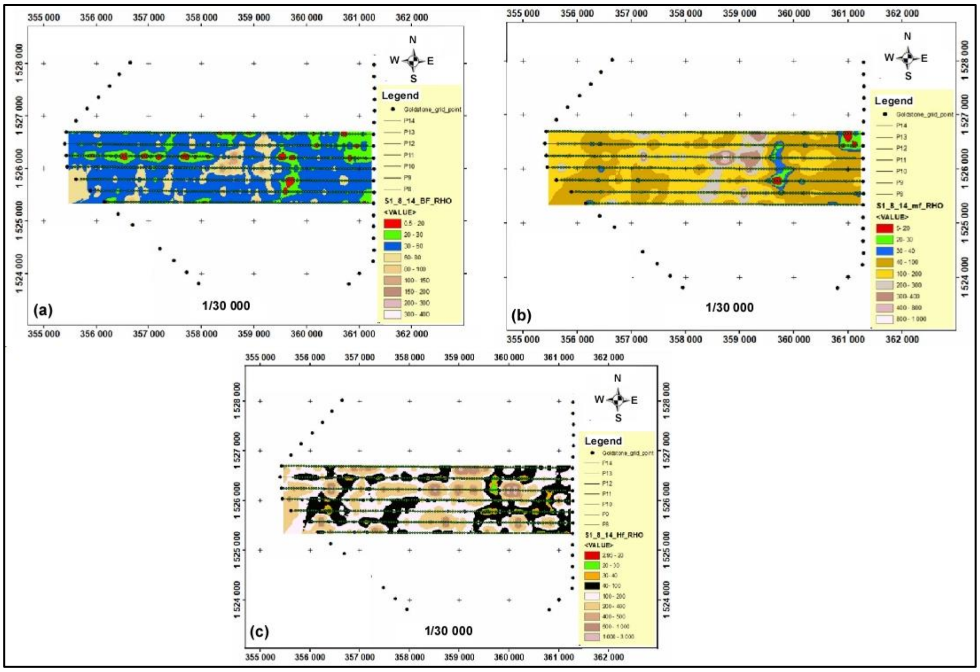

Figure 8: Resistivity anomaly map for all frequencies at Sector 1. (a) low frequencies, (b) medium frequencies, and (c) high frequencies.

To better understand the distribution of these resistivity anomalies, a 3D representation was made of the different types (low, medium, and high frequencies) (Fig. 9a). These anomalies were then superimposed on the JICA geochemical anomalies. A strong correlation between the data from this study and those from JICA was found (Fig. 9b).

Analysis of these maps reveals a certain spatial variability in the electrical resistivity data. They confirm the existence of an E-W conductive structure located on profile 12. This structure is highlighted by the low frequencies (110 and 220 Hz), which are the most penetrative (Fig. 9a). The beginnings of the profiles are marked by very low resistivity values, suggesting highly conductive units of varying depths. The presence of shallower resistive units that can be interpreted as quartz veins was also highlighted. By superimposing the various resistivity anomaly maps, it was possible to delineate zones with high mining potential in Sector 1. Thus, the following were distinguished:

- A main anomaly (Anomaly 1) N-S trending, located in the eastern end of the sector and having an area of approximately 3.5 km2 (Fig. 10);
- A secondary anomaly (Secondary Anomaly 1), N-S trending at the western end of Sector 1 and covering an area of around 2.9 km2 (Fig. 10);
- And a secondary anomaly (Secondary Anomaly 2), N-S trending in the south-central part and covering an area of about 0.96 Km2 (Fig. 10).

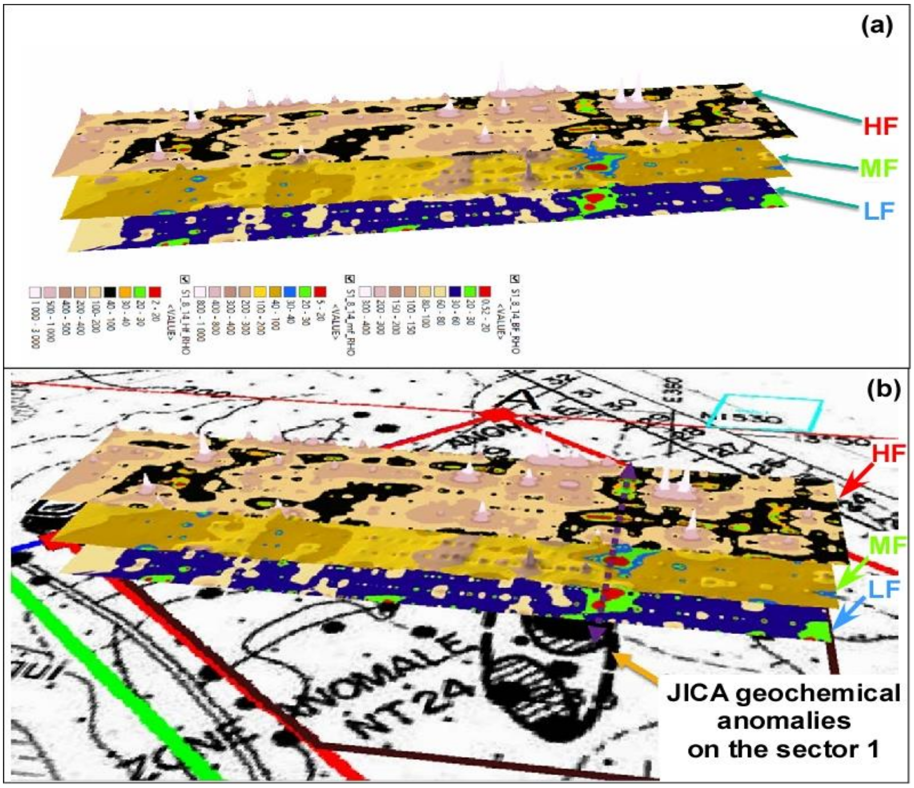

Figure 9: Map showing the superimposition of geophysical anomalies on the JICA anomalies of Sector 1.

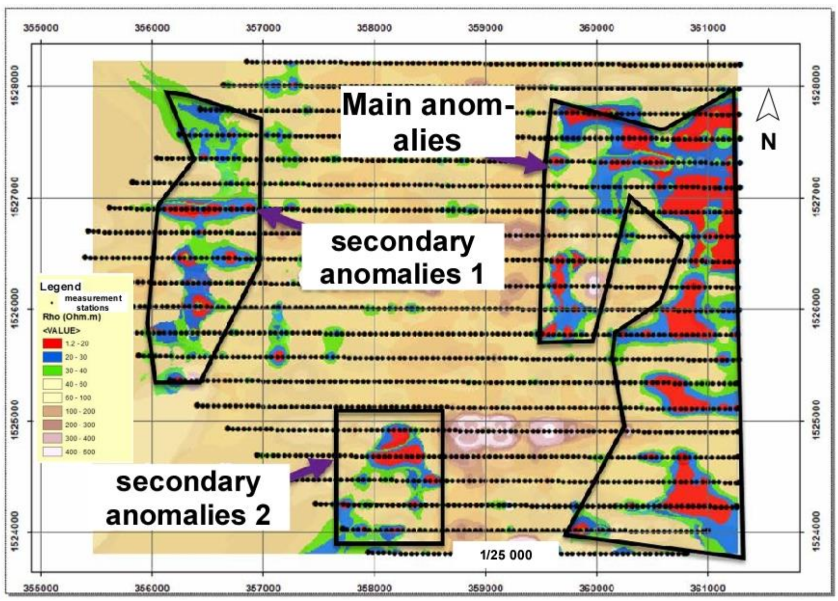

Figure 10: Resistivity map showing areas of high mining potential in Sector 1.

4.4.2 Geophysical results in Sector 2

The geophysical results for Sector 2 are presented according to resistivity values (Figs. 11, 12, and 13).

a. Layout of apparent resistivity data for low frequencies

Analysis of Figure 11 shows that at 110 Hz, the most penetrative frequency, there are many more zones with low apparent resistivity values, i.e., conductive zones, than at the other frequencies. These conductive (anomalous) zones have been grouped as follows:

Anomaly 1: covering an area of 2.33 km2, running NE-SW,

Anomaly 2: 1.24 km2 in E-W direction,

Anomaly 3: 1.47 km2 in N-S direction.

These anomalies lie directly on resistive formations (resistivity between 300 and 500 Ω·m), which can be interpreted as quartzites or quartz veins.

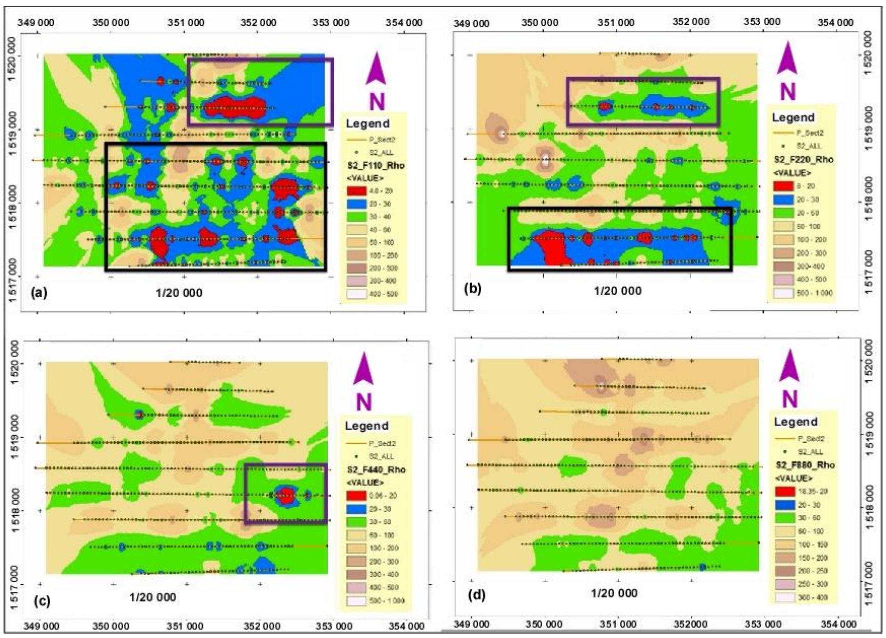

Figure 11: Low-frequency resistivity map for Sector 2.

b. Layout of apparent resistivity data for medium frequencies

The less penetrative mid-frequencies show no resistivity anomalies (Fig. 12). On the other hand, a more resistive block stands out as it gradually rises towards the surface at frequencies of 3,520 Hz (Fig. 12b), and 7040 Hz (Fig. 12c). These formations, which appear from NE to S, may correspond to resistive quartz veins (over 1,000 Ω·ms.m) or altered granite (between 300 and 500 Ω·ms.m).

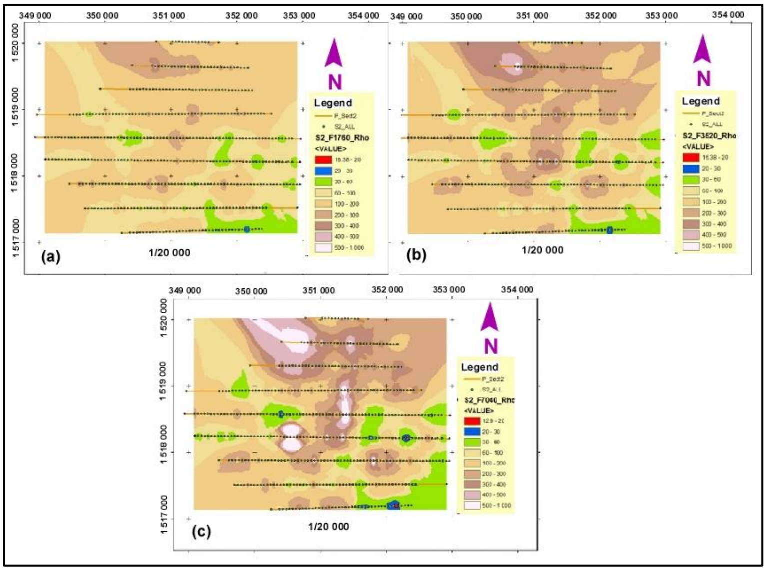

Figure 12: Mean-frequency resistivity map for Sector 2.

c. Layout of apparent resistivity data for high frequencies

For high frequencies, which are less penetrative, only frequencies 14,080 Hz and 28,520 Hz show a few conductive levels to the extreme SE for frequencies 28,520 Hz and towards the East on profiles 5 and 6 for frequencies 14,080 Hz. For frequencies 56,320 Hz, the most superficial, significant coverage of resistive to very resistive levels that can be interpreted as granite was revealed.

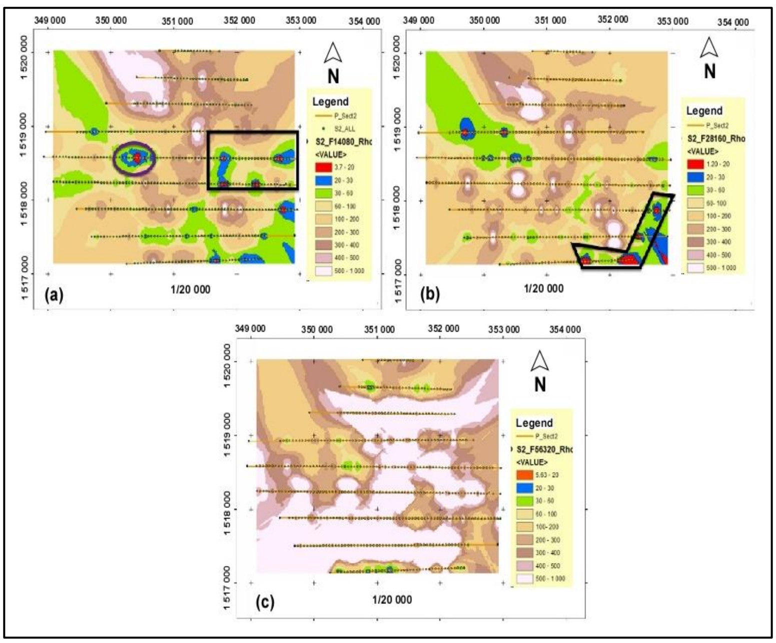

Figure 13: High-frequency resistivity map for Sector 2.

4.4.3 Geophysical results in Sector 3

In Sector 3, a form of anomaly appears over almost ¾ of the sector's total area (Fig. 14). Here, it is mainly the medium and high frequencies that highlight these anomalies (Fig. 14c&d). Two types of anomalies were highlighted:
A conductive E-W corridor, where strong resistivity anomalies for high frequencies (less penetrative and not exceeding 15 m) were highlighted, and deep anomalies of up to 50 m for low and medium frequencies in the southern and central part of Sector 3. It should be noted that some deep anomalies may be caused by the presence of fractures and weathering zones.

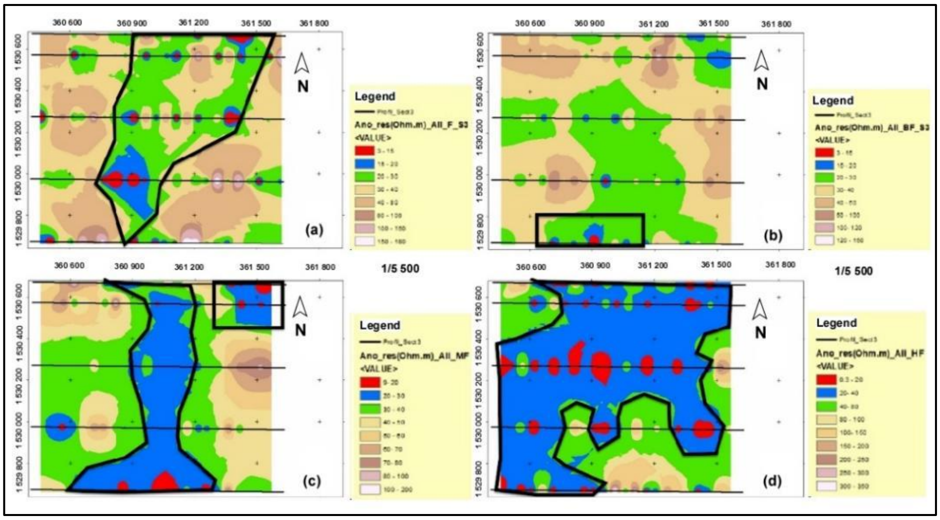

Figure 14: Resistivity anomaly map for all frequencies in Sector 3. (a) all frequencies, (b) low frequencies, (c) medium frequencies, and (d) high frequencies.

4.5 Exploration results

Compilation of previous work enabled us to target drilling sites and orient soil geochemistry. Thus, 3 types of prospecting work were carried out: rock sampling, destructive drilling holes (DDH), and soil geochemistry sampling.
Thus, the activities carried out include:

- 176 rock samples were taken over the entire study area;
- 34 RC destructive boreholes for a total meterage of 1297m, and a total number of samples taken of 653 ;
- 497 soil geochemistry samples, in 200m x 200m and 250m x 50m grids;
- 156 double samples with 200mX200m and 200mX50m grid spacing.

The main assay results for rock samples, boreholes, and soil geochemistry are presented for the various sectors of the study area. The analytical results indicate the presence of substantial gold potential in the study area.

a- Sector 1

24.06 g/t over 6m at a depth of 19-25 m,
16.24 g/t over 3m at a depth of 23-27 m,
8.06 g/t over 5m at a depth of 33-38 m,
3.18 g/t over 3m at a depth of 40-43 m.

b- Sector 2

3.75 g/t over 4m at a depth of 20-24 m,
2.24 g/t over 3m at a depth of 16-19 m.

c- Sector 3

1.46 g/t over 10m at depths of 17-27 m,
1.07 g/t over 6m at depths of 21-27 m,
1.51 g/t over 4m at depths of 10-14 m.

4.6 Mapping potential areas of gold accumulations

The compilation of field, geophysical, and geochemical data has resulted in a spatial map of the drilling points (Fig. 15). This was based on the distribution of zones with high mining potential, as highlighted by geophysical work and the results of sample analysis from the various prospecting methods. These high-potential zones correspond respectively to:

For Sector 1: the eastern part, the Western border, and the South-central part (with an overall N-S orientation).

For Sector 2: the southeastern part (NE-SW trending), the N part (EW orientation), and the centre (NS orientation).

For Sector 3: the northern part (E-W trending), the southern part (EW orientation), and the central part (EW trending).

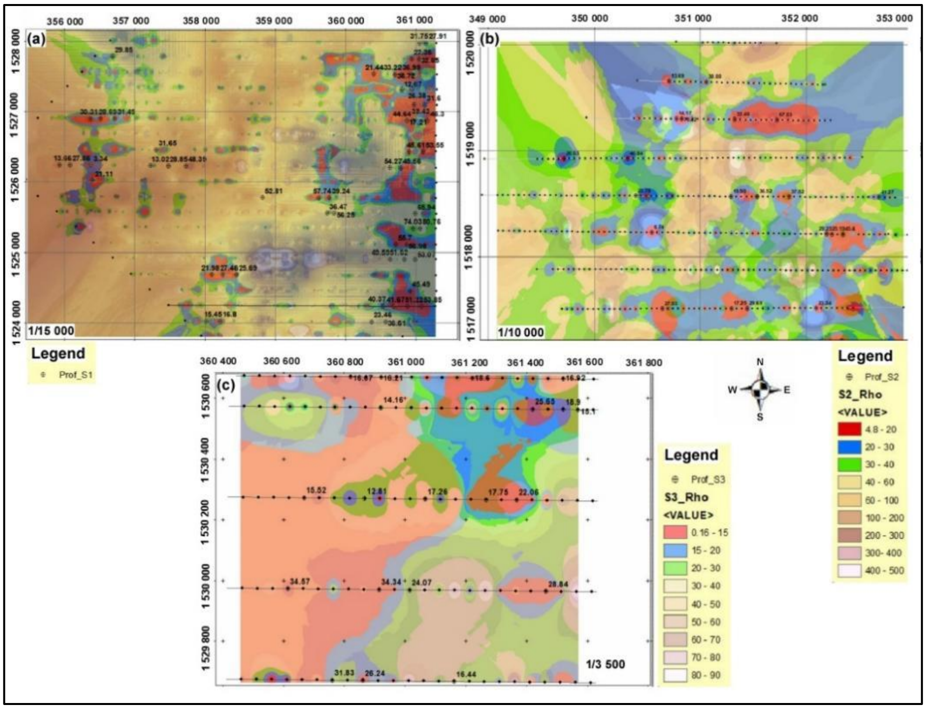

Figure 15: Map showing survey points and depths for all survey sectors. (a) Sector 1, (b) Sector 2, and (c) Sector 3.

5. Discussion

The work carried out as part of this study has revealed areas of high mining potential in various sectors investigated. Analysis of the geophysical data revealed several conductive lenses with different orientations. These anomalies coincide spatially with areas of geochemical evidence for gold mineralisation and therefore represent potential exploration targets.

Geological context. In the field, conductive lenses correspond to quartz veins, highly altered manganese schists, and acidic intrusive levels (altered granites). A similar study using a ground magnetic survey has been conducted by Echague *et al.,* (2024) in the southwest region of the Amazon Craton in Brazil. According to these authors, the analysis of magnetic anomalies on the map specifically the total gradient (TG) map reveals a linear pattern punctuated by high-frequency magnetic anomalies-oriented NNW-SSE.

In the case of the Amazon Craton study, the highest values, both in the total gradient (GT) and in the residual magnetic field (RMF), are generally associated with exposures of metasedimentary rocks from the Aguapeí Group (metarenites and metaconglomerates) containing iron oxides (magnetite, hematite and ilmenite), while the porphyritic granite of the Pindaituba Intrusive Suite exhibits low magnetic intensity, which contrasts with the metasedimentary rocks amidst a scenario of field variations. This result is in contrast with our study. In our study area, the existence of gold-panning shafts and the limited amount of drilling carried out confirm the geophysical results. Claude *et al.,* (2010) highlighted resistive levels attributed to acidic intrusive units (Granodiorite/granite) and unmineralized quartz veins. Also, Gaboury (2019), working in Boulon Djounga in Niger's Liptako has highlighted gold mineralisation in sedimentary cover, metasediments, and sulfide-rich gray quartz veins. In the West African subsurface, more than 80% of the gold extracted comes from rocks forming greenstone belts (Castaing et al., 2003). Furthermore, in Burkina Faso, Klemd et al., (1997), Klemd et al., (2002), and Castaing et al., (2003) have shown that most gold ore deposits are associated with greenstone belts or metasedimentary basins. Similar observations were made in Mali by Béziat et al., (2008), Sangaré *et al.,* (2014), and Traoré (2017); in Senegal by Dabo (2011); and in Côte d'Ivoire by Koffi *et al.,* (2022).

From a structural perspective. In this study, it has been shown that the geological structures are mainly dominated by shear zones (Fig. 5). These structures are faults, fractures, quartz veins, and large folding deduced in the studied area (Fig. 5a&b). Several fracture directions were observed, and are in the following directions: E-W, N-S, NW-SE, and NE-SW. Faults and lineations orientations are generally N-S and NW-SE, with striae azimuth N30° to N90°, dipping gently to the NE or to the E. Yechang *et al.,* (2025) show that the Heiglongjing gold deposit in China is primarily controlled by north-east trending faults and is hosted within the contact zone between Late Carboniferous granitic mylonite and syenogranite. The Yongxin gold deposit is primarily controlled by north-east trending faults and is hosted within the contact zone between Late Carboniferous granitic mylonite and syenogranite. By synthesising geological and geophysical data, these authors have highlighted the distribution of fracture structures in the Heilongjiang region. Our study revealed the presence of eight fractures. These fractures are oriented primarily along northwest, northeast, north-south, and near east-west directions.

Geophysical context. Also, the abundance of resistive units in the high-frequency map (Fig. 12d) reveals the strong meteoric alteration of the host rocks at the surface. In the field, gold-bearing conductive units are either associated with alluvium resulting from the weathering of manganese schists or generally associated with highly altered, sulphide-rich quartz veins. These units have also been identified in gold pits in sectors 1 and 3. However, the Echague *et al.,* (2024) work reveals that the regions with lower apparent resistivity background (<16,240 Ω·ms.m) are mainly associated with the occurrence of the porphyritic granite basement or hydrothermally altered metasediments, specifically where hydrothermal alteration is marked primarily by the frequent presence of iron oxides (ferruginous metarenite with magnetite and hematite). Also, areas of higher electrical resistivity (>16,240 Ω·m) are associated with exposures of metasediments from the Aguapeí Group represented by quartz-feldspar metarenites. These zones also exhibit strong hydrothermal alteration, characterised by the presence of swarms of quartz veins. These regions exhibit the highest gold concentrations within the area. Olusegun *et al.,* (2022) show, in the Kaiama sheet, that geologically, the occurrences of cassiterite and gold-bearing mineralization appear to be significantly associated with the NE-SW tectonic trend. According to Yechang *et al.,* (2025), the resistivity difference constitutes a significant geophysical indicator differentiating two types of gold mineralisation (terminal and channel). Both types of gold mineralisation are located adjacent to IP anomalies, potentially suggesting characteristics of low-sulfur gold mineralisation that are related to gradual change of physical properties of surrounding rock caused by hydrothermal solutions. The banded low magnetic anomalies in the andesite distribution area at the Alingher mining area in China reflect the demagnetization of hydrothermal alteration and indicate the existence of the alteration area. Also, in the Heilongjiang area, significant geophysical anomalies are observed at the contact zones between Late Carboniferous syenogranite and granitic mylonite, specifically within the Mesozoic Guanghua formation. These anomalies suggest that the hydrothermal breccia located around these contacts is a potential ore body site. Furthermore, the intersection of these rock types emerges as a promising mineralisation zone (Yechang *et al.,* 2025).

6. Conclusion

This study, focusing on the geophysical mapping of gold showings in the Sirba greenstone belt, specifically in the Sorbon Haoussa and Gawana areas, contributes to the identification of new drilling targets and improves geological knowledge of the area for gold mineralisation in Niger's Liptako province. It can be noted that the establishment and application of integrated geological and geophysical exploration studies can contribute as a guide for future research regarding exploration in the Niger Birimian formations. The methods and prospective exploration methods developed are part of traditional surface and relatively deep prospecting methods. This study yielded the following results:

Electromagnetic induction surveys can contribute to the geometric characterisation of gold anomalies in deep areas or near the surface.

The conductive lenses correspond to quartz veins, highly altered manganese schists, and altered granites.

The geophysical data analysis revealed that the various conductive lenses, with variable alignment, are considered areas with high potential for gold anomalies. The geophysical exploration of gold deposits in the Liptako province of Niger demonstrated the feasibility of characterising and identifying the mineralised zones. They can help to characterise the geometry of gold anomaly zones, as well as the depth and thickness of anomalous levels. This study also provides a mining guide to improve what were previously artisanal mining operations. Finally, the study shows that the Liptako province of Niger, like other parts of Africa (Burkina Faso, Ghana, and Côte d'Ivoire), harbours significant undiscovered gold potential. An exploration effort will bring this potential to light and encourage mining, which until now has remained at the artisanal stage in Niger.

Author Contributions: All authors have read and agreed to the final version of the manuscript. The corresponding author has conceived and designed the research ideas. All authors have conducted data analysis, and reviewed, and edited the drafts.
Funding: There is no external funding.
Data Availability Statement: Not applicable.
ACKNOWLEDGEMENTS. The authors wish to express their gratitude to the staff of *OM Goldstone Resources* for their collaboration in providing the data they acquired and collected, as well as for authorizing the publication of this information as an article.
Conflicts of Interest: The authors declare no conflicts of interest.

References

[1] Groves, D.I., Santosh, M. (2015). Province-scale commonalities of some world-class gold deposits: Implications for mineral exploration. Geosci. Front. 2015, 6, 389–399.

[2] Gaboury, D. (2019). Les minéralisations aurifères d'Afrique de l'Ouest: Différences et similitudes avec l'Abitibi. Technical Report. Ressources Mines et Industrie, 6, 37-42.

[3] Noura, G.R., Tourba, K., Hantchi, K.D., Hassane, B. and Konate, M. (2024). Characteristics of Gold and Its Mineralisation Style in the Boulon Djounga Eastern Perimeter of Liptako Mining Company (Central Southwestern Niger). Natural Resources, 15, 28-50. https://doi.org/10.4236/nr.2024.151003

[4] Chen, L., Wang, H., Sun, C., Chang, X., Ding, W. (2025). The Application of Integrated Geochemical and Geophysical Exploration for Prospecting Potential Prediction of Copper and Gold Polymetallic Deposits in the Fudiyingzi–Bacheli Area, Heilongjiang Province. *Minerals*, 15, 597. https://doi.org/10.3390/min15060597

[5] Harris J.R., Lafrance, B., Grunsky, E., Behnia, P., Nagizedah, M. Lawley, C. and Parsa, M. (2025). Orogenic gold mineral prospectivity mapping of the Geraldton area, Ontario: discussion of key issues. *Earth Science Informatics*, 18:360. https://doi.org/10.1007/s12145-025-01831-y

[6] Yechang, Y., Jun, C., Zhonghai, Z., Yuanjiang, Y., Chenglu, L., Haina, L., and Xiang, Z. (2025). Integrated geophysical prospecting for deep ore detection in the Yongxin gold mining area, Heilongjiang, China. Scientific report. https://doi.org/10.1038/s41598-025-92108-3

[7] Ouedraogo, Y., Ilboudo, H., Toe, W.A.B. and Naba, S. (2026). Niou Gold Deposit Structural Framework, Goren Belt, West African Craton. Open Journal of Geology, 16, 431-449. https://doi.org/10.4236/ojg.2026.167022

[8] Echague, J., Le.o-Santos, M., Melo, R., Mendes, T., Borges, W. (2024). Application of Geophysical Methods in the Identification of Mineralized Structures and Ranking of Areas for Drilling as Exemplified by Alto Guaporé Orogenic Gold Province. Minerals 2024, 14, 788. https://doi.org/10.3390/min14080788

[9] Groves, D.I., Santosh, M., Zhang, L. (2020). A scale-integrated exploration model for orogenic gold deposits based on a mineral system approach. Geosci. Front. 2020, 11, 719–738.
[10] Butterman, W. C. & Amey, E. B. (2005). Mineral Commodity Profiles, Gold. (US Geological Survey, 2005).
[11] Machens, E. (1973). Contribution à l'etude des formations du socle cristallin et de la couverture sédimentaire de l'Ouest de la République du Niger. Mémoire du BRGM, Paris.
[12] Machens, E. (1961). Prospection générale du Liptako. République du Niger. Ministère Des Travaux Publics et Des Mines. BRGM, Niamey.
[13] Soumaila, A. and Konate, M. (2005). Caractérisation de la déformation dans la ceinture birimienne (paléoprotérozoïque) de Diagorou-Darbani (Liptako nigérien, Afrique de l'Ouest). Africa Geoscience Review, 2005, 12 (3), pp.161-178. Hal-00201276v1
[14] Garba, I. (1988). The variety and possible origin of the Nigerian gold mineralisation. Okolom-dogonadji and waya veins as case studies. J. Afr. Earth Sci. (The Middle East). 7, 981-986 (1988).
[15] Pour, A. B., Hashim, M. & van Genderen, J. (2013). Detection of hydrothermal alteration zones in a tropical region using satellite remote sensing data: Bau goldfield, Sarawak, Malaysia. Ore. Geol. Rev. 54, 181–196 (2013).
[16] Boubacar Abdou, F. (2023). Apport de la télédétection et du SIG dans la cartographie des zones minéralisées : Secteurs du Sud Maradi et du Damagaram-Monio (Sud-Est Niger). Ph.D. Thesis, Université Abdou Moumouni, Niamey
[17] Gnamou, B., Ilboudo, H., Toé, W.A.B. and Sawadogo, S. (2023). Geochemical Mobility Associated to Gold and Base Metal Occurrences of Mangodara Sector, in Southern Burkina Faso, Banfora Greenstone Belts (West African Craton). Open Journal of Geology, 13, 1024-1053. https://doi.org/10.4236/ojg.2023.1310044
[18] Kearey, P., Brooks, M. and Hill, I. (2002). An Introduction to Geophysical Exploration Vol. 4 (Wiley, 2002).
[19] Dentith, M. and Mudge, S. T. (2014). Geophysics for the Mineral Exploration Geoscientist (Cambridge University Press, 2014).
[20] Projet NER/88/023. (1991). Levé géophysique aéroporté magnétique et électromagnétique-Geotem Région du Liptako. Projet NER/88/023, Compagnie Générale de Géophysique.
[21] JICA. (1993). Rapport de mission d'exploration du liptako nigérien.
[22] Bossière, G., Bonkoungou, I., Peucat, J.J. and Pupin, J.P. (1996). Origin and Age of Paleoproterozoic Conglomerates and Sandstones of the Tarkwaian Group in Burkina Faso, West Africa. Precambrian Research, 80, 153-172. https://doi.org/10.1016/S0301-9268(96)00014-9

[23] PADEM Projet. (1995). Recherche or dans le Liptako, Synthèse du Projet, Rapport final Klöckner, 1995, PADEM Projet, Ministère des Mines et de l'Énergie, 162p.
[24] Claude, J. P., and Souleymane, C. (2010). Report on drilling Tialkam Deba permits sirba belt, Liptako, Niger part 2.
[25] Kitson, A.E. (1928). Provisional Geological Map of the Gold Coast and Western Togoland: With Brief Descriptive Notes Thereon. Gold Coast Geology Survey, Bulletin, 210 p.
[26] Soumaila, A. (2000). Etude structurale, Pétrographique et Géochimique de le ceinture birimienne de Diagorou-Darbani, Liptako, Niger Occidental (Afrique de l'Ouest).Thèse, 253 p. Université de Franche-Comté, France.
[27] Abdoulwahid S. and Souley B.I. (2023). Geophysical Mapping by Electromagnetic Induction of Gold Occurrences in Birimian Formations of Liptako: Case of Sorbon Haoussa Sector (Souhwest Niger). Energy and Earth Science Vol. 6, No. 2, 2023.
[28] Rocci, G. (1965). Essai d'interprétation des mesures géochronologiques. La structure de l'Ouest Africain. Sciences de la Terre, 10, 461-478.
[29] Trompette, R. (1973). The Upper Precambrian and Lower Paleozoic of the Adrar of Mauritania (western edge of the Taoudeni Basin, West Africa). An example of craton sedimentation. Stratigraphic and sedimentological study. Earth Science Laboratory research, Marseille (St- Jérome). 1–2, 573 p. (In French).
[30] Bessoles, B. (1977). Geology of Africa: The West African Craton. BRGM. 88, 402 p. (In French).
[31] Vachette. (1986). Apport de la géochronologie isotopique à la connaissance du Protérozoïque inférieur de l'Afrique de l'Ouest. Centre international pour la formation et les échanges géologiques. 1986, Num 10, pp 25-44 ; Geological sketch map.
[32] Palacky, G. J. (1987). Resistivity Characteristics of Geologic Targets. In M. N. Nabighian (Ed.), Electromagnetic Methods in Applied Geophysics Theory: Tulsa, Okla (Vol. 1, pp. 53-122). Society of Exploration Geophysicists
[33] Perrouty, S., Aillères, L., Jessell, M.W., Baratoux, L., Bourassad, Y., and Crawford, B. (2012). Revised Eburnean Geodynamic Evolution of the Gold-Rich Southern Ashanti Belt, Ghana, with New Field and Geophysical Evidence of Pre-Tarkwaian Deformations. Precambrian Research, 204-205, 12-39. https://doi.org/10.1016/j.precamres.2012.01.003
[34] Naba, S., Lompo, M., Debat, P., Bouchez, J.L. and Béziat, D. (2004). Structure and Emplacement Model for Late-Orogenic Paleoproterozoic Granitoids: The Tenkodogo-Yamba Elongate Pluton (Eastern Burkina Faso). Journal of African Earth Sciences, 38, 41-57. https://doi.org/10.1016/j.jafrearsci.2003.09.004

[35] Miningou, M.Y.W., Affaton, P., Meunier, J.D., et al., (2017). Establishment of a lithostratigraphic column in the Béli area (Northeastern Burkina Faso, West Africa) based on the occurrence of a glacial triad and a molassic sequences in Neoproterozoic sedimentary formations. Implications for the Pan-African orogeny. Journal of African Earth Sciences. 131, 80–97. DOI: https://doi.org/10.1016/j.jafrearsci.2017.03.016.
[36] Konate, M., Ahmed, Y., Gartner, A.D., Alzouma, A.H., Ibrahim, M., Tourba, K., Hofmann, M., Zieger, J. and Linnemann, U. (2018). U-Pb Detrital Zircon Ages of Sediments from the Firgoun and Niamey Areas (Eastern Border of West African Craton, West Niger). Comptes Rendus Geoscience, 350, 267-278. https://doi.org/10.1016/j.crte.2018.06.005
[37] Garba Saley, H., Konaté, M. and Okunlola, O.A. (2024). Petrographic Study of Mn-bearing Gondite (Birimian) of Téra Area in the Leo-Man Shield (West African Craton) in Niger. Korea Economic and Environmental Geology. 57, 25–39. DOI: https://doi.org/10.9719/EEG.2024.57.1.25
[38] Naba, S. (2007). Propriétés magnétiques et caractères structuraux des granites du Burkina Faso oriental (Craton Ouest Africain, 2,2-2,0 Ga): Implications géody-namiques. Ph.D. Thesis, Université de Toulouse-Paul SABATIER.
[39] Kouamelan, A.N. (1996). Géochronologie et Géochimie des Formations Archéennes et Protérozoïques de la Dorsale de Man en Côte d'Ivoire. Implications pour la Transition Archéen-Protéozoïque. https://tel.archives-ouvertes.fr/tel-00653760
[40] Lompo, M. (2009). Geodynamic Evolution of the 2.25-2.0 Ga Palaeoproterozoic Magmatic Rocks in the Man-Leo Shield of the West African Craton. A Model of Subsidence of an Oceanic Plateau. Geological Society, London, Special Publications, 323, 231-254. https://doi.org/10.1144/sp323.11
[41] Ama Salah, I. (1991). Pétrographie et relations structurales des formations metavolcaniques et sédimentaires du Birimien du Niger occidental. Problème de l'accrétion crustale au paléoprotérozoique inférieur. Ph.D. Thesis, Université d'Orléans, Orléans.
[42] Castaing, C., Billa, M., Milesi, J.P., Thiéblemont, D., Le Metour, J., Egal, E., Donzeau, M., Guerrot, C., Cocherie, C., Chevremont, P., Tegyey, M., Itard, Y., Zida, B., Ouedraogo, I, Kote, S., Kabore, B.E., Ki, J.C. and Zunino, C. (2003). Notice explicative de la carte géologique et minière au 1/1 000 000e du Burkina Faso. Edition du BRGM, Paris.
[43] Klemd, R. and Ott, S. (1997). Compositional Characteristics of Fluid Inclusions as Exploration Tool for Au-Mineralisation at Larafella, Burkina Faso. Journal of Geochemical Exploration, 59, 251-258. https://doi.org/10.1016/S0375-6742(97)00012-5.
[44] Klemd, R., Hunken, U. and Olesh, M. (2002). Metamorphism of the Country Rocks Hosting Gold—Sulfide-Bearing Quartz Veins in the Paleoproterozoic Southern Kibi-Winneba Belt (SE-Ghana). Journal of African Earth Sciences, 35, 199-211.

[45] Béziat, D., Dubois, M., Debat, P., Nikie, S., Salvi, S. and Tollon, F. (2008). Gold Metallogeny in the Birimian Craton of Burkina Faso (West Africa). Journal of African Earth Sciences, 50, 215-233.

[46] Sangaré, A., Driouch, Y., Salvi, S. et al., (2014). Geology of Kalana late-Eburnean Gold Deposit (Birimian, Southwestern Mali). Bulletin de l'institut Scientifique: Rabat, Section Sciences de la Terre, 1, 85-108.

[47] Traore, D.Y. (2017). Etude metallogenique du district aurifere de Syama (Mali): Analyse comparative de gisements situes sur une meme structure lithospherique eburneenne. Ph.D. Thesis, Universite de Toulouse, Toulouse.

[48] Dabo, M. (2011). Tectonique et minéralisations aurifères dans les formations birimiennes de Frandi-Boboti, boutonnière de Kédougou-Kéniéba, Sénégal. Ph.D. Thesis, Université de Rennes 1, Rennes.

[49] Koffi, A.Y., Thébaud, N., Kouamelan, A.N., Baratoux, L., Bruguier, O., Vanderhaeghe, O., Pitra, P., Kemp, A.I.S. and Evans, N.J. (2022). Archean to Paleoproterozoic Crustal Evolution in the Sassandra-Cavally Domain (Côte d'Ivoire, West Africa): Insights from Hf and U-Pb Zircon Analyses. Precambrian Research, 382, Article ID: 106875. https://doi.org/10.1016/j.precamres.2022.106875

[50] Olusegun, O, I., Andongma, W, T., Rafiu, B, B., Jiriko, N, G., and Mohammed, D.A. (2022). Spatial mapping of hydrothermal alterations and structural features for gold and cassiterite exploration.
http://creativecommons.org/licenses/by-nc-nd/4.0/